**Molecular Human Reproduction, Vol.18, No.3 pp. 111–120, 2012**
Advanced Access publication on October 16, 2011 doi:10.1093/molehr/gar068

MHR Basic science of reproductive medicine

ORIGINAL RESEARCH

# Human Fallopian tube epithelium constitutively expresses integrin endometrial receptivity markers: no evidence for a tubal implantation window

**J.K. Brown [1], J.L.V. Shaw [2], H.O.D. Critchley [1], and A.W. Horne [1,*]**

[1]MRC Centre for Reproductive Health, The University of Edinburgh, Queen's Medical Research Institute, 47 Little France Crescent, Edinburgh EH16 4TJ, UK

*Correspondence address. Tel: +44-131-242-6609; Fax: +44-131-242-6441; E-mail: andrew.horne@ed.ac.uk

*Submitted on July 11, 2011; resubmitted on October 4, 2011; accepted on October 5, 2011*

**ABSTRACT:** Understanding of ectopic implantation within the Fallopian tube (FT) is limited. In the human uterus, the putative 'window of implantation' in the mid-luteal phase of the menstrual cycle is accompanied by increased endometrial epithelial expression of the integrins $\alpha_1\beta_1$, $\alpha_4\beta_1$ and $\alpha_v\beta_3$ and its ligand osteopontin. Similar cyclical changes in FT integrin expression have been proposed to contribute to ectopic implantation, but supporting data are limited. In the current study, we present quantitative data on human FT transcription and translation of the integrin subunits $\alpha_1$, $\alpha_4$, $\alpha_V$, $\beta_1$ and $\beta_3$ during the follicular and mid-luteal phases of the menstrual cycle, together with a supporting immuocytochemical analysis of their spatial distribution within the FT, and that of osteopontin. In contrast to previous studies, our data indicate that all five integrin receptivity markers are constitutively transcribed and translated in the FT, with no evidence for changes in their expression or distribution during the window of implantation in the mid-luteal phase of the cycle. Furthermore, we could find no evidence for cyclic redistribution of the integrin $\alpha_v\beta_3$ ligand osteopontin within the FT. Although we do not rule out the involvement of integrin endometrial receptivity markers in the establishment of ectopic pregnancy, our findings do not support their differential expression during a tubal implantation window.

**Key words:** ectopic pregnancy / Fallopian tube / integrin / receptivity / implantation

## Introduction

An ectopic pregnancy is defined as any pregnancy implanted outside the uterus, with the vast majority (>98%) occurring in the Fallopian tube (FT) (Varma and Gupta, 2009; Sivalingam *et al.*, 2011). The condition has a major clinical and socioeconomic impact worldwide and remains the leading cause of death in the first trimester of pregnancy in the developed world (Farquhar, 2005; Varma and Gupta, 2009). In developing countries, it has been estimated that 10% of women admitted to hospital with a diagnosis of ectopic pregnancy ultimately die from the condition (Leke *et al.*, 2004).

The etiology of tubal implantation is still far from complete, but the bulk of the existing literature supports the hypothesis that it arises from a combination of impaired embryo-tubal transport and changes in the FT environment (Shaw *et al.*, 2010; Brown and Horne, 2011). In the uterus, implantation only occurs when the endometrium is receptive during a putative 'window of implantation' in the mid-luteal phase of the menstrual cycle that is associated with marked changes in integrin expression within the endometrial epithelium (Lessey, 1998). The integrins are a family of widely expressed heterodimeric cell surface receptors that mediate cell–cell and cell–extracellular matrix adhesion and, in doing so, regulate many aspects of cell behavior including survival, proliferation, migration and differentiation. Twenty-four different integrin heterodimers are currently recognized in humans, each comprising a pair of non-covalently associated α- and β-subunits (Barczyk *et al.*, 2010). In addition to providing a physical transmembrane link between the extracellular environment and the cytoskeleton, they are capable of transducing bi-directional signals across the cell membrane (Hynes, 2002).

In humans, endometrial transcription of integrins $\alpha_4$, $\alpha_v$, $\beta_1$ and $\beta_3$ is significantly higher during the mid-luteal phase of the menstrual cycle, compared with the follicular phase, with the $\alpha_v$ and $\beta_3$ subunits

showing the largest increases in expression (Dou et al., 1999). More specifically, the $\beta_3$ subunit and osteopontin, a ligand for integrin $\alpha_v\beta_3$, are only expressed at the luminal surface of the endometrium during the receptive period (Lessey et al., 1992; Apparao et al., 2001) supporting the concept that this cycle-dependent protein is involved in implantation in humans (Lessey, 1998).

While endometrial epithelial expression of the integrin heterodimers, $\alpha_1\beta_1$, $\alpha_4\beta_1$ and $\alpha_v\beta_3$, correlates with receptivity to the presenting embryo in humans (Lessey et al., 1992, 1994a; Lessey, 1998), functional data pertaining to the role of these integrins in implantation is currently limited. Homozygous integrin $\beta_1$ and $\alpha_4$ null mutations are embryonic lethal (Fassler and Meyer, 1995; Stephens et al., 1995; Yang et al., 1995), while ~80% of $\alpha_v$ null/null mice die *in utero*, with the remainder dying shortly after birth (Bader et al., 1998). Consequently, there is no data on implantation in female mice that are homozygous null for these three integrins. Homozygous integrins $\alpha_1$ null mice are viable but do not exhibit any reduction in fecundity, suggesting that this integrin does not contribute to implantation in the mouse model (Gardner et al., 1996). The phenotype of integrin $\beta_3$ knockout mice is more complex, with female homozygous null mice producing ~50% smaller litters due to a combination of embryo and placental defects (Hodivala-Dilke et al., 1999). No direct analysis of implantation defects has been undertaken in the $\beta_3$ knockout mice but implantation has been shown to be inhibited in another mouse model by functional blockade of integrin $\alpha_v\beta_3$ using neutralizing monoclonal antibodies against integrin $\beta_3$ and integrin $\alpha_v$ or the specific $\alpha_v\beta_3$ disintegrin echistatin (Illera et al., 2000).

A 'window of implantation' has also been proposed to occur in the FT, during which time the tubal epithelium is susceptible to ectopic implantation (Sulz et al., 1998). If such a window does occur in the FT, it follows that the integrins $\alpha_1\beta_1$, $\alpha_4\beta_1$ and $\alpha_v\beta_3$ are likely to be differentially expressed within the FT during the follicular and mid-luteal phases of the menstrual cycle. Semi-quantitative RT–PCR data suggest that the integrin subunits $\alpha_1$, $\alpha_v$ and $\beta_3$ are differentially regulated across the oestrous cycle in the bovine oviduct, with expression levels reaching a minima during the late-luteal phase before, in the case of $\beta_3$, peaking in the pre-ovulation phase (Gabler et al., 2003). Human studies have also produced data in support of this hypothesis, specifically, reporting increased immunohistochemical labeling intensity for the $\beta_3$ subunit (Sulz et al., 1998) and more recently the $\alpha_v\beta_3$ heterodimer (Makrigiannakis et al., 2009) in human tubal epithelium during the mid-luteal phase of the cycle. However, both of these studies were based entirely on immunohistochemistry observations and, given the potential key role for integrin $\alpha_v\beta_3$ in embryo implantation (Illera et al., 2000), there is a requirement for a quantitative analysis of integrin receptivity marker expression across the menstrual cycle in human FT. The current study was undertaken with the aim of meeting this objective.

# Materials and Methods

## Tissue collection

Full thickness cross sections of human FT ampulla (follicular phase $n = 6$, mid-luteal phase $n = 6$) and Pipelle™ uterine endometrial biopsies (follicular phase $n = 2$, mid-luteal phase $n = 2$) were collected from fertile women (Parity ≥2) with regular menstrual cycles (24–35 days) during hysterectomy for benign gynecological conditions (median age = 41; range 27–49 years). Tissues were collected into RNAlater (Applied Biosystems, Warrington, UK) and neutral-buffered formalin, as previously described (Shaw et al., 2011). Menstrual cycle dating was determined by three criteria, each of which had to correlate in order for inclusion in the study: (i) date of last menstrual period (as reported by the patient); (ii) staging by an expert gynecological pathologist of an endometrial biopsy obtained at the time of FT biopsy and (iii) serum estradiol (follicular phase >100 pM) and progesterone (follicular phase <10 nM; mid-luteal >20 nM). Approval for this study was obtained from the Lothian Research Ethics Committee (04/S1103/20, 05/S1103/14, 07/S1103/29), and informed, written consent was obtained from each patient.

## Quantitative reverse transcription PCR

RNA was extracted from tissue using TRIzol reagent (Invitrogen, Paisley, UK), treated with DNase and purified using RNeasy kits (Qiagen, Crawley, UK). Two hundred nanograms of RNA were reverse-transcribed into cDNA using random hexamers, according to the recommended method (Applied Biosystems). TaqMan quantitative real-time reverse transcription PCR (qRT-PCR) was used to quantify integrin transcript levels. Specific primers were designed using the Universal Probe Library (UPL) Assay Design Center (www.roche-applied-science.com) and used in conjunction with UPL probes (Roche Applied Science). Details of primer sequences and probes used are given in Table I. Reactions were performed, in triplicate, under standard conditions in an ABI Prism 7900 instrument (Applied Biosystems). Integrin gene expression was normalized to ribosomal 18S expression, using the $2^{-\Delta\Delta C_t}$ method, and expressed as relative to a positive standard (a single cDNA sample from follicular FT, included on each reaction plate).

**Table I qRT-PCR primer and probe sequences.**

| | |
|---|---|
| ITGA1 forward | 5′-AATTGGCTCTAGTCACCATTGTT-3′ |
| ITGA1 reverse | 5′-CAAATGAAGCTGCTGACTGGT-3′ |
| ITGA1 UPL probe (FAM) | 14 |
| ITGA4 forward | 5′-GGAATATCCAGTTTTTACACAAAGG-3′ |
| ITGA4 reverse | 5′-AGAGAGCCAGTCCAGTAAGATGA-3′ |
| ITGA4 UPL probe (FAM) | 57 |
| ITGAV forward | 5′-GCCGTGGATTTCTTCGTG-3′ |
| ITGAV reverse | 5′-GAGGACCTGCCCTCCTTC-3′ |
| ITGAV UPL probe (FAM) | 64 |
| ITGB1 forward | 5′-CGATGCCATCATGCAAGT-3′ |
| ITGB1 reverse | 5′-ACACCAGCAGCCGTGTAAC-3′ |
| ITGB1 UPL probe (FAM) | 65 |
| ITGB3 forward | 5′-GGGCAGTGTCATGTTGGTAG-3′ |
| ITGB3 reverse | 5′-CAGCCCCAAAGAGGGATAAT-3′ |
| ITGB3 UPL probe (FAM) | 13 |
| 18S forward | 5′-CGGCTACCACATCCAAGGAA-3′ |
| 18S reverse | 5′-GCTGGAATTACCGCGGCT-3′ |
| 18S probe (VIC) | 5′-TGCTGGCACCAGACTTGCCCTC-3′ |

## Quantitative dual chemiluminescent western blot

RNAlater stabilized samples of FT were homogenized in pH 8.0 lysis buffer (50 mM Tris–HCl; 150 mM NaCl; 1 mM EDTA; 1% Triton-X100, 1% Na-deoxycholate; EDTA-free complete mini protease inhibitors [Roche Diagnostics, Welwyn Garden City, UK) and 1 mM of the serine protease inhibitor, AEBSF (Sigma, Poole, UK)] using a TissueLyser bead mill (Qiagen). Protein quantification was performed by using the Bradford Assay (Bradford, 1976), adapted for the Cobas Fara centrifugal analyzer (Roche Diagnostics) and samples adjusted to 2 mg/ml total protein in lysis buffer, before further 1:1 dilution in 2× NuPAGE LDS sample buffer (Invitrogen) containing 100 mM dithiothreitol (Sigma). One-dimensional gel electrophoresis was performed in 15-well NuPAGE 4–12% Bis–Tris gels (Invitrogen) using 5–25 μg of total protein/lane alongside SeeBlue® Plus2 prestained molecular weight standards (Invitrogen). A positive control (pooled protein extracts from follicular FT biopsies) was also included in every gel to allow intra-blot comparisons to be made. Gels were equilibrated for 15 min in transfer buffer (50 mM Tris, 40 mM Glycine and 0.05% SDS), before blotting at 20 V (limited to 80 mA/gel) onto polyvinylidene fluoride membrane (Immobilon P: Millipore, Livingston, UK) in the presence of transfer buffer + 10% methanol using a Transblot SD (Bio-Rad Laboratories, Hemel Hempstead, UK).

Blots were blocked for 30 min in TBS-T20 (pH 7.4 Tris-buffered saline containing 0.5% Tween 20) + 2% Marvel (Premier Foods, St Albans, UK) and incubated for 2 h with combinations of mouse and rabbit anti-integrin (Abcam, Cambridge, UK), anti-β actin primary antibodies and/or negative control antibodies (Sigma) diluted appropriately in TBS-T20 + 2% Marvel (Table II). Blots were then washed in TBS-T20 (6 × 3 min) and incubated for 1 h with the appropriate combination of horse-radish peroxidase (HRPO) and alkaline phosphatase (ALKP)-conjugated secondary antibodies (Stratech Scientific, Newmarket, UK) diluted to 20 ng/ml in TBS-T20 + 2% Marvel (Table II). Following washing in TBS-T20 (6 × 3 min), integrin-specific HRPO labeling was visualized using Chemiluminescent Peroxidase Substrate-1 (Sigma). Blots were then washed (3 × 5 min) in TBS-T20 and rinsed in 100 mM Tris–HCl + 100 mM NaCl (pH 9.5), before β-actin-specific ALKP labeling was visualized using CDP-STAR Star (Boehringer-Mannheim, Germany). Images were acquired using a VersaDoc™ Imaging System (Bio-Rad Laboratories). Integrin-specific HRPO chemiluminescent signal and β-actin-specific ALKP chemiluminescent signal were measured using ImageJ software (Rasband, 1997–2011). After normalizing against β-actin, values for integrin-specific labeling were expressed as relative to the positive control. After imaging, blots were stained with Imperial Protein Stain (Fisher Scientific UK, Loughborough, UK) to confirm uniform blotting efficiency.

## Immunocytochemistry

Formal-saline fixed paraffin wax embedded (FFPE) sections were mounted on Snow Coat X-tra™ charged slides (Surgipath Europe, Peterborough, UK), dewaxed in xylene and rehydrated through graded ethanol. Antigen retrieval was performed by pressure cooking, from cold, for 5 min at pressure in 10 mM Tris, 1 mM EDTA and 0.05% T20 (pH 9.0). Once the pressure cooker had returned to ambient pressure, slides were washed in deionized water ($DH_2O$) and endogenous peroxidase activity blocked by a 30-min incubation in TBS-T20 containing 1% $H_2O_2$. Slides were washed in TBS-T20 and transferred to a Sequenza immunostaining centre (Thermo Shandon; Runcorn, UK). Non-specific protein binding was blocked by incubating sections for 30 min with staining buffer [TBS-T20 + 10% normal horse serum for integrin labeling or TBS-T20 + 4% bovine serum albumin (BSA) of osteopontin and fibronectin labeling].

For immunohistochemistry (IHC): samples were incubated overnight at 4°C with primary anti-integrin antibodies and controls diluted appropriately in staining buffer (Table III). Slides were subsequently washed in TBS-T20 and incubated for 10 min at room temperature with staining buffer, before being incubated for 30 min with ImmPRESS Universal Antibody (anti-mouse Ig/anti-rabbit Ig, peroxidase) Polymer Detection Kit (Vector Laboratories, Peterborough, UK). Sections were washed in TBS-T20 and incubated for 10 min with 3,3′-diaminobenzidine + Chromogen (Dako UK, Ely, UK), counterstained in Mayer's Haematoxylin and mounted with No. 1.5 glass coverslips using Pertex (Cellpath PLC, Hemel Hempstead, UK).

For paired immunofluorescence (IF): endogenous biotin was blocked using an avidin/biotin blocking kit (Vector Laboratories). After washing in TBS-T20, samples were incubated for 1 h at room temperature with primary anti-integrin-$\beta_3$-specific antibody or control rabbit immunoglobulin G (IgG) diluted appropriately in staining buffer (Table III). Sections were then washed and incubated for 1 h at room temperature with staining buffer containing 2 μg/ml of biotinylated goat anti-rabbit IgG (Vector Laboratories). Sections were washed and incubated with R.T.U. ABC Reagent (Vector Laboratories), as per the manufacturer's instructions,

**Table II Antibodies used in dual chemiluminescent western blots.**

| Integrin antibody | Working conc./ dilution | Loading control antibody | Loading control working conc. | Donkey secondary antibodies |
|---|---|---|---|---|
| Monoclonal mouse $IgG_1$ anti-integrin $\alpha_1$ | 0.2 μg/ml | Rabbit anti-β actin | 0.2 μg/ml | Anti-mouse HRPO<br>Anti-rabbit ALKP |
| Control Mouse $IgG_1$ | 0.2 μg/ml | Rabbit anti-β actin | 0.2 μg/ml | Anti-mouse HRPO<br>Anti-rabbit ALKP |
| Monoclonal rabbit anti-integrin $\alpha_4$ | 1 in 10 000 | Mouse anti-β actin | 1 in 10 000 | Anti-mouse ALKP<br>Anti-rabbit HRPO |
| Monoclonal rabbit anti-integrin $\beta_1$ | 1 in 10 000 | Mouse anti-β actin | 1 in 10 000 | Anti-mouse ALKP<br>Anti-rabbit HRPO |
| Polyclonal rabbit anti-integrin $\beta_3$ | 0.2 μg/ml | Mouse anti-β actin | 1 in 10 000 | Anti-mouse ALKP<br>Anti-rabbit HRPO |
| Control Rabbit IgG | 0.2 μg/ml | Mouse anti-β actin | 1 in 10 000 | Anti-mouse ALKP<br>Anti-rabbit HRPO |

before further washing and incubation for 5 min with Tyramide Signal Amplification (TSA) plus FITC (PerkinElmer, Seer Green, UK). To elute existing antibody-peroxidase complexes from the sections, slides were removed from the Sequenza immunostaining center, microwaved at full power in pre-warmed 10 mM sodium citrate (pH 6.0) for 6 min and allowed to cool to room temperature. Slides were then returned to the Sequenza immunostaining center and blocked with staining buffer followed by the avidin/biotin blocking kit. After washing, samples were incubated for 1 h at room temperature with primary anti-osteopontin-specific antibody or control mouse $IgG_{2a}$ diluted appropriately in staining buffer (Table III). Sections were then washed and incubated for 1 h at room temperature with staining buffer containing 2 μg/ml of biotinylated rabbit anti-mouse IgG (Dako). After washing, sections were incubated with R.T.U. ABC Reagent, before further washing and incubation for 5 min with TSA plus Cy3 (PerkinElmer). Finally, sections were washed with TBS and counter stained for 15 min in 1 μM ToPro-3 (Invitrogen) in TBS, before mounting with No. 1.5 glass coverslips using Mowiol (pH 8.5) mounting media (EMD Biosciences, San Diego, CA, USA). Fluorescent images were acquired with a LSM510 META confocal microscope equipped with a ×63 Plan-Apochromat® 1.4 NA objective lens (Carl Zeiss, Welwyn Garden City, UK).

**Table III Integrin antibody working concentrations for immunocytochemistry.**

| Primary antibody | Supplier | IHC conc. | IF conc. |
|---|---|---|---|
| Monoclonal mouse $IgG_1$ anti-integrin $\alpha_1$ (FB12) | Chemicon | 0.5 μg/ml | — |
| Monoclonal mouse $IgG_1$ anti-integrin $\alpha_v\beta_3$ (BV3) | Abcam | 2–0.5 μg/ml | 2–0.5 μg/ml |
| Monoclonal mouse $IgG_1$ anti-integrin $\alpha_v\beta_3$ (23C6) | Chemicon | 2–0.5 μg/ml | 2–0.5 μg/ml |
| Monoclonal mouse $IgG_1$ anti-integrin $\alpha_v\beta_3$ (LM609) | Chemicon | 2–0.5 μg/ml | 2–0.5 μg/ml |
| Monoclonal mouse $IgG_{2a}$ anti-osteopontin (53) | Abcam | 0.2 μg/ml | 0.2 μg/ml |
| Monoclonal rabbit IgG anti-integrin $\alpha_4$ (EPR1355Y) | Abcam | 1 in 3000 | — |
| Polyclonal rabbit IgG anti-integrin $\alpha_V$ | Abcam | 0.5 μg/ml | — |
| Monoclonal rabbit IgG anti-integrin $\beta_1$ (EP1041Y) | Abcam | 1 in 3000 | — |
| Monoclonal rabbit IgG anti-fibronectin (F1) | Abcam | 1 in 5000 | 1 in 10 000 |
| Polyclonal rabbit IgG anti-integrin $\beta_3$ | Abcam | 0.5 μg/ml | 0.2 μg/ml |
| Control mouse $IgG_1$ | Serotec | 2–0.5 μg/ml | — |
| Control mouse $IgG_{2a}$ | Abcam | 0.2 μg/ml | 0.2 μg/ml |
| Control rabbit IgG | Vector | 1–0.2 μg/ml | 0.5–0.2 μg/ml |

## Statistical analysis

All statistical analyses were performed using InStat (GraphPad Software, La Jolla, CA, USA). Differences between groups were analyzed using a two-tailed, Mann–Whitney test and differences were considered significant when $P < 0.05$.

# Results

## Quantitative RT–PCR analysis of integrin endometrial receptivity marker gene transcription in follicular and mid-luteal-staged FT biopsies

Messenger RNA transcripts from all five integrin subunit genes studied (ITGA1, ITGA4, ITGAV, ITGB1 and ITGB3) were detected by qRT-PCR in human FT biopsies (Fig. 1). There was little evidence for differences in integrin transcript levels between the follicular and mid-luteal FT groups. Although median ITGB3 transcript levels were higher in the mid-luteal group, the spread of the data and statistical analysis (Mann–Whitney: $P = 0.1797$) indicate that this observation occurred by chance and that there is no difference in ITGB3 expression between the two groups. With the exception of ITGA4, which appears to be transcribed at lower levels (Fig. 1C), FT (Fig. 1: clear plots) expression of all of the integrins studied here appears to be commensurate with that observed in mid-luteal endometrium (Fig. 1: filled plots).

## Quantitative western blot analysis of integrin endometrial receptivity marker protein levels in follicular and mid-luteal staged FT biopsies

Integrin-$\alpha_1$-, $\alpha_4$-, $\beta_1$- and $\beta_3$-specific antibodies reacted with discreet bands in western blots of pooled protein extracts from both follicular and mid-luteal FT biopsies (Fig. 2). No bands were detected with integrin-$\alpha_v$-specific antibodies at total protein loadings of up to 25 μg/lane. Integrin-$\alpha_1$-specific antibodies reacted strongly with a band of ~190 KDa (expected: 200 KDa), and to a much lesser extent with a band of ~85 KDa, at a total protein loading of 10 μg/lane. Integrin-$\alpha_4$-specific antibodies reacted with a band of ~85 KDa (expected: 150 KDa) at a total protein loading of 25 μg/lane. Integrin-$\beta_1$-specific antibodies reacted strongly with a band of ~90 KDa (expected size: 88 KDa) at a total protein loading of 5 μg/lane. Integrin-$\beta_3$-specific antibodies reacted with a band of ~75 KDa (expected size: 87 KDa), and to a lesser extent ~45 KDa, at a total protein loading of 25 μg/lane. No bands were observed when integrin-specific antibodies were replaced with equivalent amounts of control mouse $IgG_1$ or control rabbit IgG (data not shown).

Data derived from quantitative analysis of dual chemiluminescent western blots of individual FT protein extracts are presented in Fig. 3. Integrated density values of integrin $\alpha_1$, $\alpha_4$, $\beta_1$ and $\beta_3$ bands were normalized against that of β-actin bands for each lane and the result expressed as a function of the positive control (pooled protein extracts from follicular FT biopsies). There was no evidence for differences in integrin protein levels between the follicular and mid-luteal staged samples.

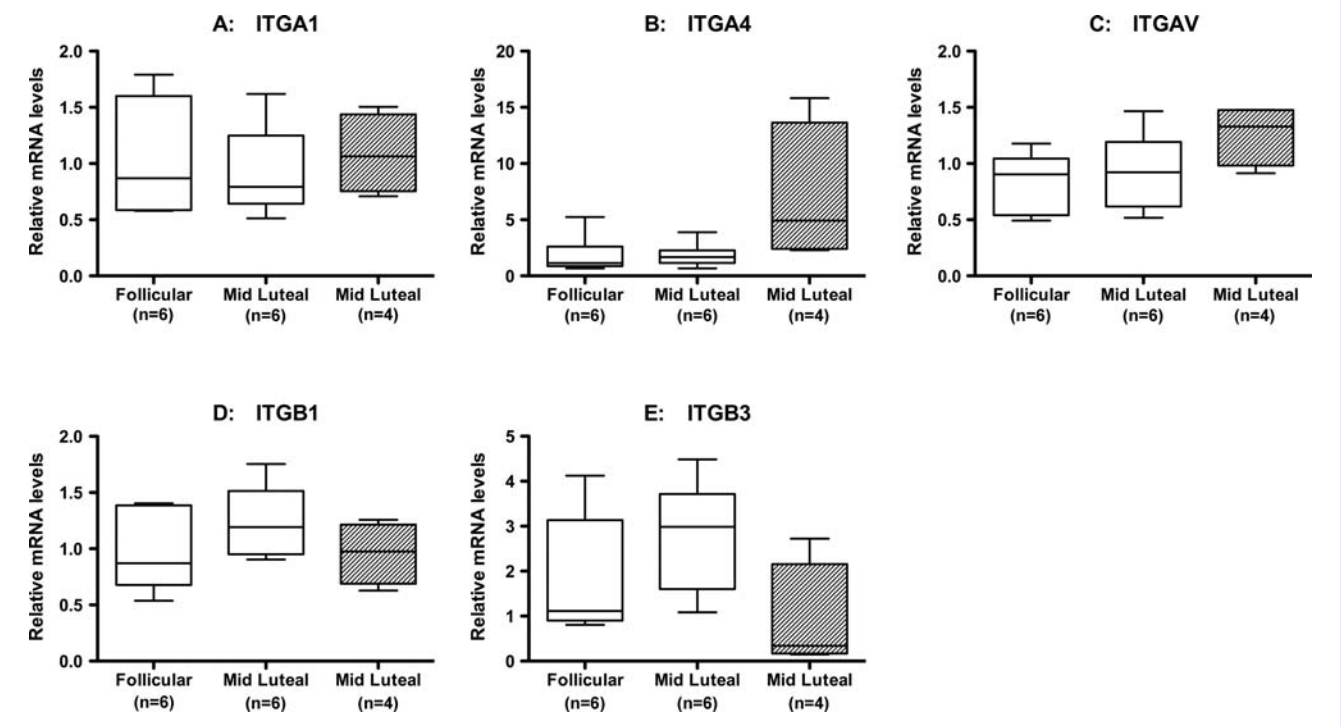


**Figure 1** Quantitative RT–PCR analysis of integrin transcripts in FT (open plots) and endometrial (filled plots) biopsies taken during the follicular and mid-luteal phases of the menstrual cycle. Boxes represent median values ± 1 SD, whiskers denote the full range of the data. Individual panels are presented for: (**A**) ITGA1; (**B**) ITGA4; (**C**) ITGAV; (**D**) ITGB1 and (**E**) ITGB3. No significant ($P > 0.05$) differences in integrin expression were observed between follicular and mid-luteal FT biopsies.

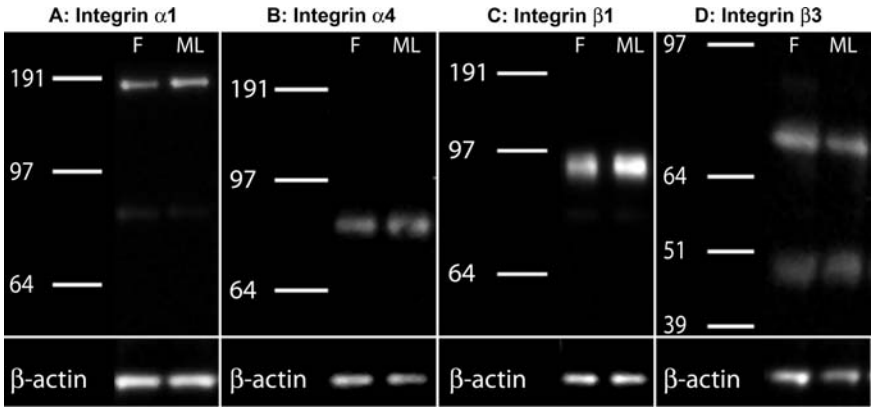


**Figure 2** Images of dual chemiluminescent western blots for integrins and β-actin in pooled protein extracts from follicular (F) and mid-luteal (ML) FT biopsies. Separate panels are shown for: (**A**) mouse ($IgG_1$) anti-integrin $\alpha_1$; (**B**) rabbit anti-integrin $\alpha_4$; (**C**) rabbit anti-integrin $\beta_1$ and (**D**) rabbit anti-integrin $\beta_3$. Images of β-actin specific labeling are provided in the lower panels.

## Immunolocalization of integrin endometrial receptivity markers in follicular and mid-luteal-staged FT biopsies

Representative images of follicular ($n = 6$) and mid-luteal ($n = 6$) FT tissue sections labeled with integrin-specific antibodies are shown in Fig. 4. Antigen retrieval at pH 9.0 (10 mM Tris, 1 mM EDTA, 0.05% T20) allowed detection of all five integrin subunits under investigation and the integrin $\alpha_v\beta_3$ ligands, osteopontin and fibronectin, without significant degradation of tissue morphology. Blocking of non-specific protein binding using BSA produced superior results for fibronectin and osteopontin, compared with normal serum, which contains

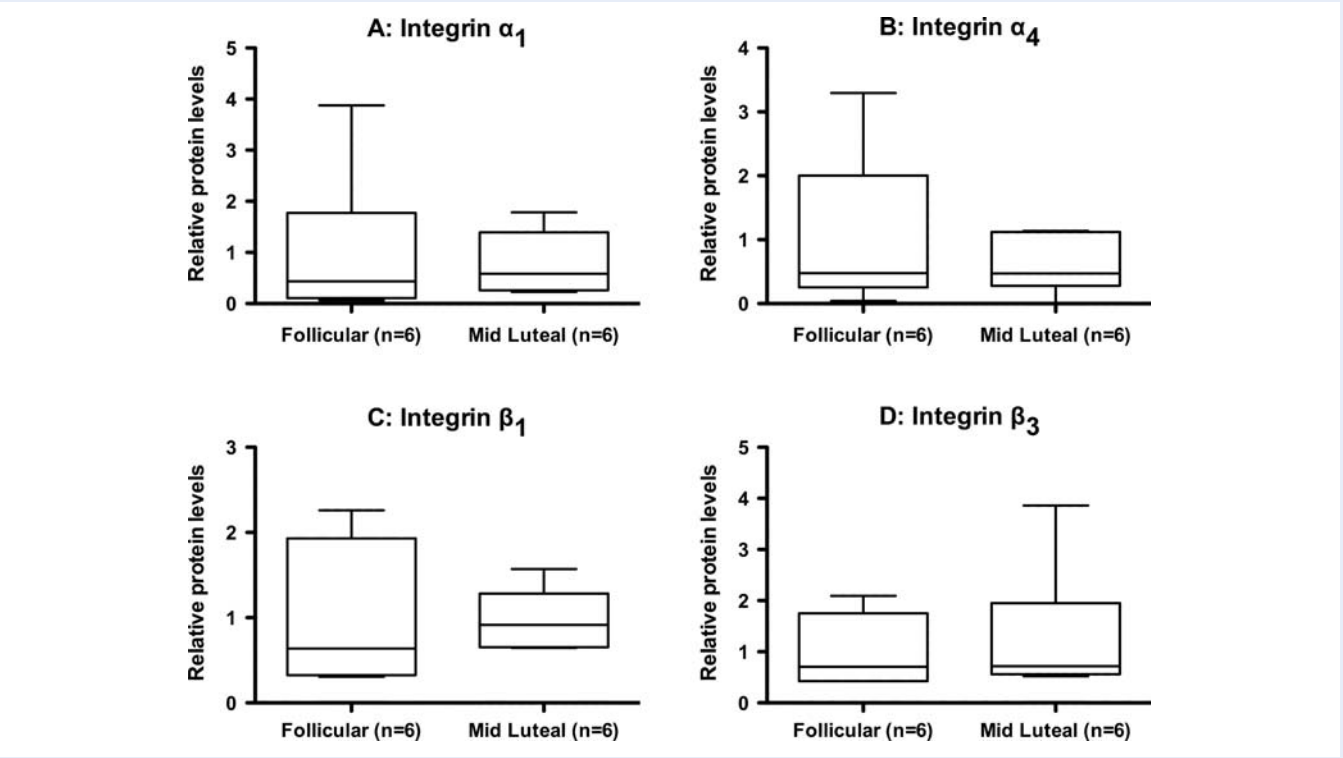


**Figure 3** Quantitative analysis of integrin protein levels in follicular and mid-luteal FT protein extracts. Boxes represent median values ± 1 SD, whiskers denote the full range of the data. Individual panels are presented for: (**A**) integrin $\alpha_1$; (**B**) integrin $\alpha_4$; (**C**) integrin $\beta_1$ and (**D**) integrin $\beta_3$. No significant ($P > 0.05$) differences in integrin expression were observed between follicular and mid-luteal phases of the menstrual cycle.

significant levels of both proteins (Mosesson and Amrani, 1980; Scatena *et al.*, 2007). None of the monoclonal antibodies directed against the integrin $\alpha_v\beta_3$ heterodimer (BV3; 23C6 or LM609) produced convincing specific labeling of FFPE sections, even when highly sensitive TSA labeling was employed. The epitope recognized by the polyclonal rabbit anti-integrin $\alpha_v$ (Fig. 4C) was methanol sensitive, even when quenching of endogenous peroxidase using 0.3% $H_2O_2$ in methanol was performed prior to antigen retrieval.

There was no evidence for changes in integrin labeling intensity, or distribution, between follicular and mid-luteal staged sections of FT (Fig. 4A–E). Similarly, specific labeling of the integrin $\alpha_v\beta_3$ ligands osteopontin (Fig. 4F) and fibronectin (Fig. 4G) was not influenced by the phase of the cycle in the FT. Integrins $\alpha_4$ (Fig. 4B), $\alpha_v$ (Fig. 4C) and $\beta_1$ (Fig. 4D) specific immunohistochemistry produced intense labeling throughout the FT epithelium, in a pattern consistent with their presence at the plasma membrane, whereas integrin-$\beta_3$-specific labeling was largely restricted to the luminal plasma membrane of epithelial cells (Fig. 4E). All four of these integrins were detected on leukocytes scattered throughout the FT stromal or, in the case of integrin $\beta_3$ (Fig. 4E), located near the basement membrane of the epithelium. There was also evidence for the expression of integrins $\alpha_4$, $\alpha_v$ and $\beta_1$ by endothelial cells and, in the case of the $\alpha_v$ and $\beta_1$ subunits, by smooth muscle cells within the FT stroma and surrounding connective tissue. By contrast, integrin-$\alpha_1$-specific labeling was restricted to epithelial cells and exhibited an intense punctuate distribution consistent with it being restricted to the golgi body, with no evidence for it being expressed on the cell surface (Fig. 4A). Osteopontin specific labeling was widely distributed throughout the FT and surrounding smooth muscle and connective tissues but was most prominent within the epithelium compartment of the mucosa, where it appeared to be expressed at high levels by a subset of epithelial cells (Fig. 4F). Although also widely distributed, fibronectin specific labeling was not present with the epithelium of the FT and was largely restricted to endothelial cells and blood pool in the stroma (Fig. 4G). Non-specific labeling was not observed when specific antibodies were substituted with equivalent amounts of appropriate control IgG (Fig. 4C1–C4).

## Paired immunofluorescent labeling of integrin $\beta_3$ and osteopontin in follicular and mid-luteal-staged FT and endometrial biopsies

Further analysis of integrin $\beta_3$ and osteopontin co-expression was undertaken using paired immunofluorescence. Representative images of follicular and mid-luteal FT ($n = 6$ per group) and endometrium ($n = 2$ per group) tissue sections are shown in Fig. 5. There was limited osteopontin- and integrin-$\beta_3$-specific labeling in the endometrial epithelia during the follicular phase of the menstrual cycle, with intense $\beta_3$ specific labeling of sporadic cells within the stromal compartment (Fig. 5A), but both molecules were strongly expressed in the luminal epithelium of mid-luteal-staged endometrium (Fig. 5A*). In contrast, FT epithelial cells co-expressed integrin $\beta_3$ and osteopontin during both the follicular (Fig. 5B) and mid-luteal (Fig. 5B*) phases of the cycle, with no evidence for any cycle-dependent changes in expression level

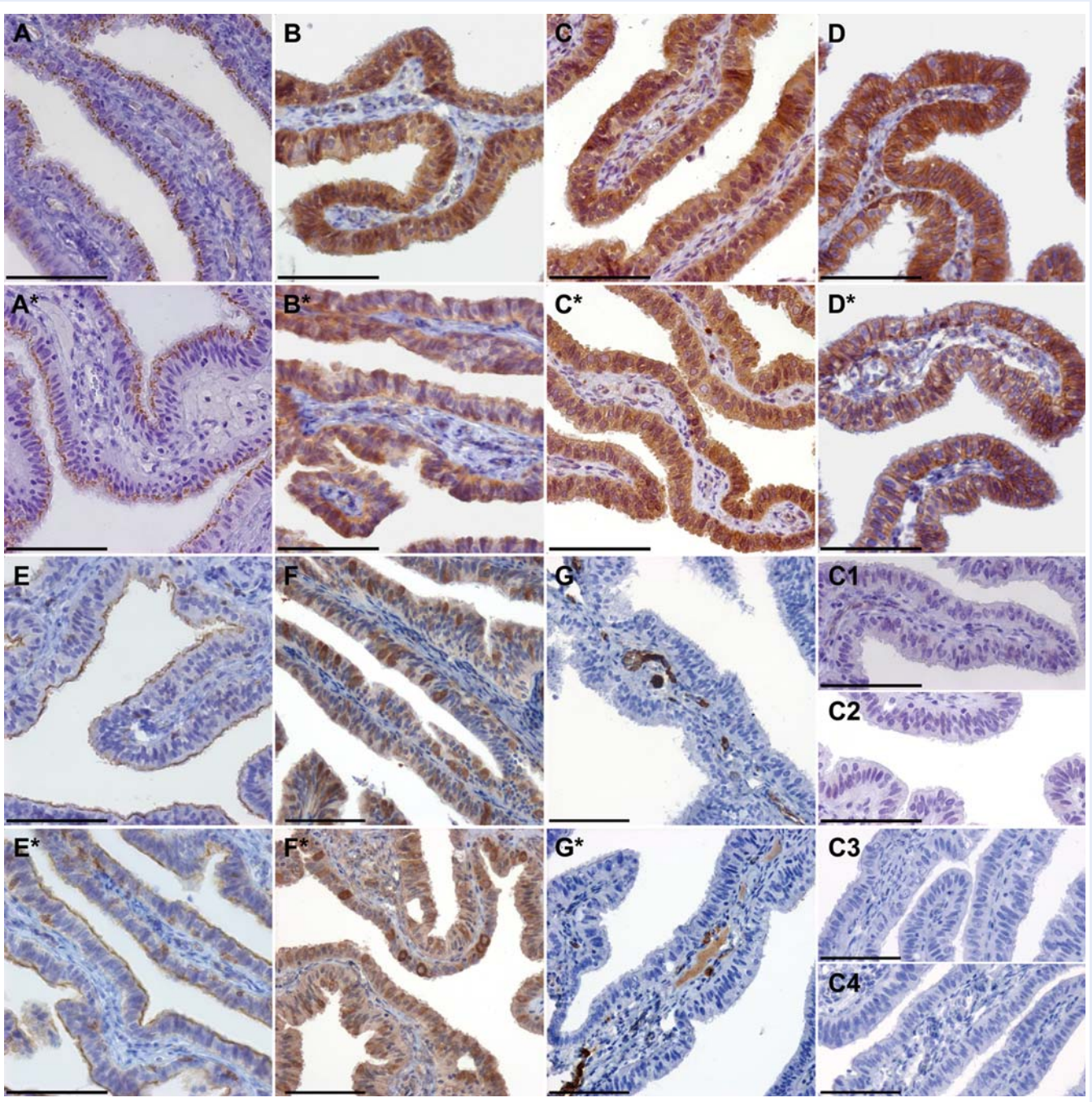


**Figure 4** Distribution of integrin subunits and putative integrin $\alpha_V\beta_3$ ligands within FT biopsies from the follicular and mid-luteal (asterisk) phases of the menstrual cycle. Panels show representative images of tissue sections labeled with: (**A**) mouse ($IgG_1$) anti-integrin $\alpha_1$; (**B**) rabbit anti-integrin $\alpha_4$; (**C**) rabbit anti-integrin $\alpha_V$; (**D**) rabbit anti-integrin $\beta_1$; (**E**) rabbit anti-integrin $\beta_3$; (**F**) mouse ($IgG_{2a}$) anti-osteopontin and (**G**) rabbit anti-fibronectin. Staining fidelity was confirmed by substituting primary antibodies with equivalent amounts of: (**C1**) control mouse $IgG_1$ (integrin staining run); (**C2**) control rabbit IgG (integrin staining run); (**C3**) control mouse $IgG_{2a}$ (osteopontin staining run); control rabbit IgG (fibronectin staining run). Scale bars represent 100 μm.

or spatial distribution. Despite being co-expressed in the epithelia of FT and mid-luteal endometria, there was very limited evidence for co-localization (1.4NA objective: ~200 nm lateral//~400 nm axial resolution for Cy3) of integrin $\beta_3$ and osteopontin in either tissue. Integrin $\beta_3$ also exhibited a different intracellular distribution in the FT and endometrial epithelia, with the vast majority of specific labeling occurring at or near the luminal surface of FT epithelial cells (Fig. 5B and B*). No evidence for non-specific labeling or crosstalk was observed when specific antibodies were substituted with equivalent amounts of control IgG (Fig. 5C1 and C2).

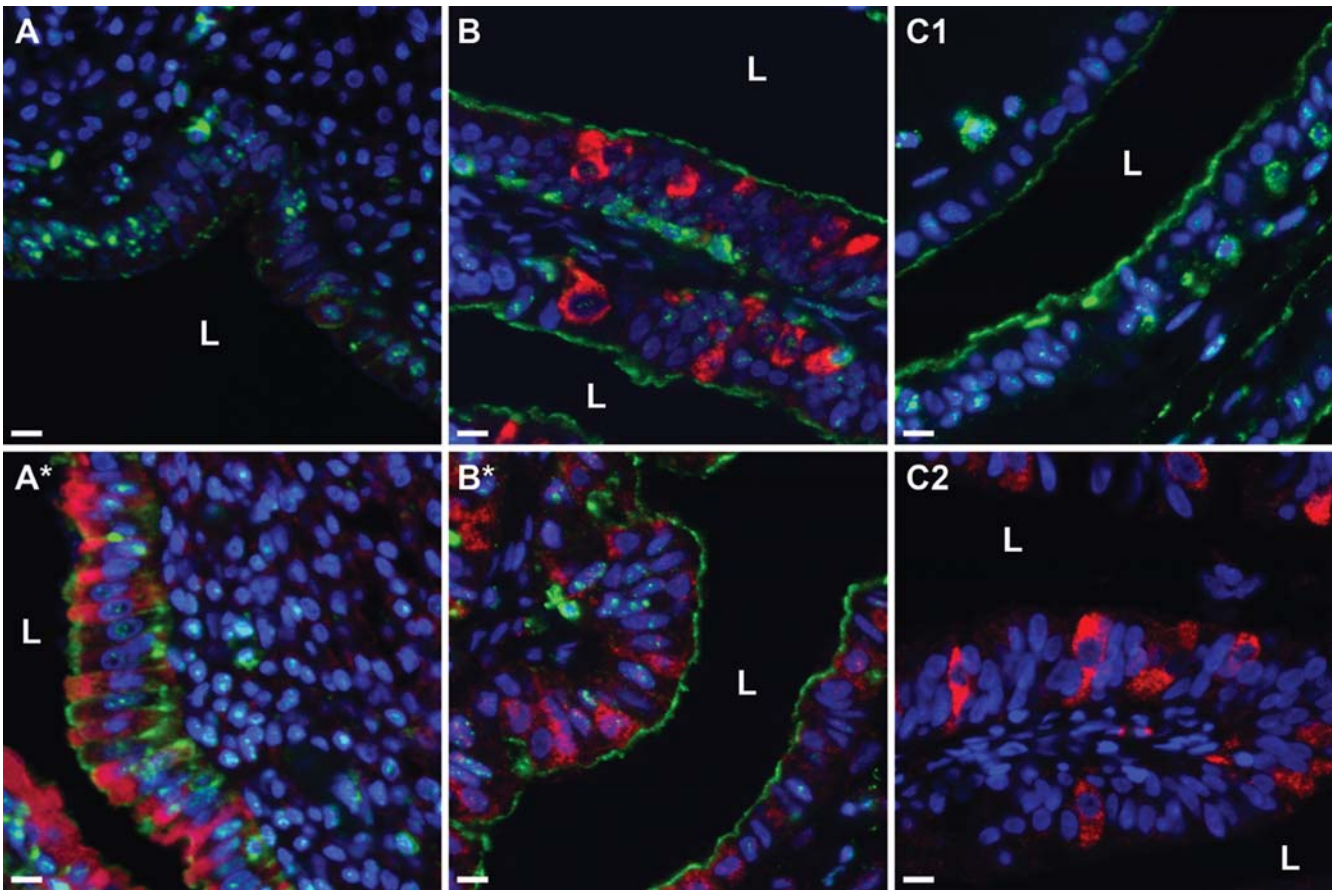


**Figure 5** Paired immunofluorescent labeling of integrin $\beta_3$ and osteopontin within endometrial (A/A*) and FT (B/B*) biopsies from the follicular (**A** and **B**) and mid-luteal (**A*** and **B***) phases of the menstrual cycle. (A/A*) and (B/B*) show representative images of tissue sections labeled with rabbit anti-integrin $\beta_3$ (green), mouse anti-osteopontin (red) and TopPro-3 nuclear counterstain (blue). Staining fidelity was confirmed on sections of mid-luteal FT, substituting mouse anti-osteopontin (**C1**) or rabbit anti-integrin $\beta_3$ (**C2**) with equivalent amounts of control antibodies. Excitation and exposure settings were standardized from each tissue. L indicates the luminal side of the epithelium. Scale bars represent 10 μm.

## Discussion

To date, published data on integrin receptivity marker expression in human FT has been limited to semi-quantitative immunohistochemical studies (Sulz *et al.*, 1998; Makrigiannakis *et al.*, 2009). Here, we present quantitative data on human FT transcription (Fig. 1) and translation (Fig. 3) of the integrin subunits $\alpha_1$, $\alpha_4$, $\alpha_V$, $\beta_1$ and $\beta_3$ during the follicular and mid-luteal phases of the menstrual cycle, together with comprehensive supporting immunocytochemistry data (Figs 4 and 5). In contrast to previous studies (Sulz *et al.*, 1998; Makrigiannakis *et al.*, 2009), our data indicate that all five integrin receptivity markers ($\alpha_1$, $\alpha_4$, $\alpha_V$, $\beta_1$ and $\beta_3$) are constitutively transcribed and translated in the FT epithelium, with no evidence for changes in their expression or distribution during the putative window of implantation in the mid-luteal phase of the cycle.

Our data are at variance with two previous immunohistochemical studies that reported increased integrin $\beta_3$ subunit (Sulz *et al.*, 1998) and $\alpha_v\beta_3$ heterodimer (Makrigiannakis *et al.*, 2009)-specific antibody labeling in the epithelium of the FT during the mid-luteal phase of the menstrual cycle, with little or no labeling of the same area during the follicular phase. While it could be argued that this discrepancy arises from differences in the specificity of the antibodies used, the rabbit polyclonal antibody used in the current study produced results entirely consistent with published data for the temporal/spatial distribution of integrin $\beta_3$ (Lessey *et al.*, 1992, 1994a) and $\alpha_v\beta_3$ (Tei *et al.*, 2003) in the endometrium (Fig. 5A and A*). Furthermore, the staining pattern we obtained with rabbit polyclonal anti-integrin $\beta_3$ on FFPE sections of mid-luteal-staged endometrium (Fig. 5A*) was identical to that previously described for a monoclonal mouse integrin $\alpha_v\beta_3$ heterodimer-specific antibody (clone LM609) in frozen sections of mid-luteal endometrium (Tei *et al.*, 2003). In the current study, both qRT-PCR (Fig. 1) and western blot (Figs 2 and 3) analysis were undertaken on tissue extracts derived from whole cross-sections of FT and it could be argued that subtle changes in epithelial expression of the integrin subunits could be overlooked against background expression in surrounding tissues. Indeed, the integrin subunits $\beta_1$ and $\alpha_V$ are 'promiscuous', forming heterodimmers with multiple partners, and are both expressed by a wide variety of cells,

including smooth muscle and stromal cells (Hynes, 2002; Barczyk *et al.*, 2010). However, their partners ($\alpha_1$, $\alpha_4$, and $\beta_3$) are much more restricted in their distribution, which is predominantly epithelial in the FT and we are confident that any significant changes in epithelial expression of their functional heterodimmers ($\alpha_1\beta_1$, $\alpha_4\beta_1$ and $\alpha_v\beta_3$) would be detected by the measuring $\alpha_1$, $\alpha_4$, and $\beta_3$ in whole FT cross-sections. It should be noted that Dou *et al.* (1999) were able to detect significantly higher transcription of the integrin subunits $\alpha_4$, $\alpha_v$, $\beta_1$ and $\beta_3$ during the mid-luteal phase of the menstrual cycle, compared with the follicular phase, using conventional RT–PCR to interrogate cDNA from unfractionated endometrial biopsies.

The absence of cycle-dependent changes in expression of integrin receptivity markers and osteopontin in human FT, reported in the current study, contrasts with the situation in endometrium (Lessey *et al.*, 1992, 1994a; Lessey, 1998; Dou *et al.*, 1999; Apparao *et al.*, 2001). We would argue that this indicates that expression of these receptivity markers, in particular integrin $\alpha_v\beta_3$ and osteopontin, is likely to be regulated through different mechanisms in the endometrium and the FT. In addition, the intracellular distribution of the $\alpha$1 and $\beta_3$ subunits also differ markedly between the epithelia of the FT (Figs 4 and 5) and the endometrium (Lessey *et al.*, 1992), suggesting that these integrins may also fulfill functionally distinct roles in the two tissues. This is, perhaps, unsurprising given the likely evolutionary disadvantage of a FT that is receptive to ectopic implantation at any point during the menstrual cycle, let alone one that increases its receptivity to compete with the endometrium during the window of implantation.

The current study is not the first to report differential regulation of gene expression in the FT and endometrium. We have previously shown that, unlike endometrium, FT constitutively expresses the estrogen receptor isoform ER$\alpha$ throughout the menstrual cycle, with no evidence for a reduction in expression during the mid-luteal phase, when the tissue is exposed to peak levels of circulating progesterone (Horne *et al.*, 2009). These differences in gene regulation are consistent with the distinct embryonic origins of the FT and uterus, and the persistence of differential Hox gene expression in the two organs after birth (Taylor *et al.*, 1997). This spatial Hox axis, more typical of embryonic tissue, is thought play a role in preserving the developmental plasticity of the female reproductive system throughout the menstrual cycle and during pregnancy, allowing tissue remodeling to be differentially regulated in the FT and uterus by steroid hormones (Taylor *et al.*, 1997; Masse *et al.*, 2009).

Defects in integrin $\beta_3$ expression have been implicated in the pathology of endometriosis, luteal phase defects and polycystic ovarian syndrome (Lessey *et al.*, 1992, 1994b), all of which are associated with infertility or pregnancy loss. Although we do not rule out the involvement of integrin receptivity markers in the establishment of ectopic pregnancy, our data do not support the hypothesis that the temporal/spatial expression profile of integrin receptivity markers ($\alpha_1\beta_1$, $\alpha_4\beta_1$ and $\alpha_v\beta_3$) or the integrin $\alpha_v\beta_3$ ligand, osteopontin, reported in endometrium is mirrored in FT. Nor do they support the existence of a window of implantation in the FT. It would, therefore, appear that integrin expression is regulated through different mechanisms in the FT and endometrium, opening up the future possibility of being able to selectively modulate integrin receptivity marker expression in the FT without disturbing normal intrauterine implantation.

## Authors' roles

J.K.B. design, experiments, analysis and interpretation, drafting article and final approval. J.L.V.S. experiments and final approval. H.O.D.C. revising for critical content and final approval. A.W.H. conception and design, interpretation, revising for critical content and final approval.

## Acknowledgements

We are grateful to Catherine Murray, Sharon McPherson and Helen Dewart for patient recruitment.

## Funding

This study was supported by the Medical Research Council (MRC G0802808). Funding to pay the Open Access publication charges for this article was provided by the Medical Research Council (MRC G0802808).

## Conflict of interest

J.K.B. and J.L.V.S. have nothing to declare. A.W.H. and H.O.D.C. hold a UK patent for a diagnostic biomarker for ectopic pregnancy (#0712801.0). A.W.H. is supported by the UK Medical Research Council (2009–13) and an Albert McKern Bequest (2010–11).

## References

Apparao KB, Murray MJ, Fritz MA, Meyer WR, Chambers AF, Truong PR, Lessey BA. Osteopontin and its receptor alphavbeta(3) integrin are coexpressed in the human endometrium during the menstrual cycle but regulated differentially. *J Clin Endocrinol Metab* 2001;**86**:4991–5000.

Bader BL, Rayburn H, Crowley D, Hynes RO. Extensive vasculogenesis, angiogenesis, and organogenesis precede lethality in mice lacking all alpha v integrins. *Cell* 1998;**95**:507–519.

Barczyk M, Carracedo S, Gullberg D. Integrins. *Cell Tissue Res* 2010; **339**:269–280.

Bradford MM. A rapid and sensitive method for the quantitation of microgram quantities of protein utilizing the principle of protein-dye binding. *Anal Biochem* 1976;**72**:248–254.

Brown JK, Horne AW. Laboratory models for studying ectopic pregnancy. *Curr Opin Obstet Gynecol* 2011;**23**:221–226.

Dou Q, Williams RS, Chegini N. Expression of integrin messenger ribonucleic acid in human endometrium: a quantitative reverse transcription polymerase chain reaction study. *Fertil Steril* 1999; **71**:347–353.

Farquhar CM. Ectopic pregnancy. *Lancet* 2005;**366**:583–591.

Fassler R, Meyer M. Consequences of lack of beta 1 integrin gene expression in mice. *Genes Dev* 1995;**9**:1896–1908.

Gabler C, Chapman DA, Killian GJ. Expression and presence of osteopontin and integrins in the bovine oviduct during the oestrous cycle. *Reproduction* 2003;**126**:721–729.

Gardner H, Kreidberg J, Koteliansky V, Jaenisch R. Deletion of integrin alpha 1 by homologous recombination permits normal murine development but gives rise to a specific deficit in cell adhesion. *Dev Biol* 1996;**175**:301–313.

Hodivala-Dilke KM, McHugh KP, Tsakiris DA, Rayburn H, Crowley D, Ullman-Cullere M, Ross FP, Coller BS, Teitelbaum S, Hynes RO. Beta3-integrin-deficient mice are a model for Glanzmann

thrombasthenia showing placental defects and reduced survival. *J Clin Invest* 1999;**103**:229–238.

Horne AW, King AE, Shaw E, McDonald SE, Williams AR, Saunders PT, Critchley HO. Attenuated sex steroid receptor expression in fallopian tube of women with ectopic pregnancy. *J Clin Endocrinol Metab* 2009; **94**:5146–5154.

Hynes RO. Integrins: bidirectional, allosteric signaling machines. *Cell* 2002; **110**:673–687.

Illera MJ, Cullinan E, Gui Y, Yuan L, Beyler SA, Lessey BA. Blockade of the alpha(v)beta(3) integrin adversely affects implantation in the mouse. *Biol Reprod* 2000;**62**:1285–1290.

Leke RJ, Goyaux N, Matsuda T, Thonneau PF. Ectopic pregnancy in Africa: a population-based study. *Obstet Gynecol* 2004;**103**:692–697.

Lessey BA. Endometrial integrins and the establishment of uterine receptivity. *Hum Reprod* 1998;**13**(Suppl 3):247–258; discussion 259–261.

Lessey BA, Damjanovich L, Coutifaris C, Castelbaum A, Albelda SM, Buck CA. Integrin adhesion molecules in the human endometrium. Correlation with the normal and abnormal menstrual cycle. *J Clin Invest* 1992;**90**:188–195.

Lessey BA, Castelbaum AJ, Buck CA, Lei Y, Yowell CW, Sun J. Further characterization of endometrial integrins during the menstrual cycle and in pregnancy. *Fertil Steril* 1994a;**62**:497–506.

Lessey BA, Castelbaum AJ, Sawin SW, Buck CA, Schinnar R, Bilker W, Strom BL. Aberrant integrin expression in the endometrium of women with endometriosis. *J Clin Endocrinol Metab* 1994b;**79**:643–649.

Makrigiannakis A, Karamouti M, Petsas G, Makris N, Nikas G, Antsaklis A. The expression of receptivity markers in the fallopian tube epithelium. *Histochem Cell Biol* 2009;**132**:159–167.

Masse J, Watrin T, Laurent A, Deschamps S, Guerrier D, Pellerin I. The developing female genital tract: from genetics to epigenetics. *Int J Dev Biol* 2009;**53**:411–424.

Mosesson MW, Amrani DL. The structure and biologic activities of plasma fibronectin. *Blood* 1980;**56**:145–158.

Rasband WS. *Image J*. Bethesda, MD, USA: U. S. National Institutes of Health, 1997–2011. http://imagej.nih.gov/ij/.

Scatena M, Liaw L, Giachelli CM. Osteopontin: a multifunctional molecule regulating chronic inflammation and vascular disease. *Arterioscler Thromb Vasc Biol* 2007;**27**:2302–2309.

Shaw JL, Dey SK, Critchley HO, Horne AW. Current knowledge of the aetiology of human tubal ectopic pregnancy. *Hum Reprod Update* 2010;**16**:432–444.

Shaw JL, Wills GS, Lee KF, Horner PJ, McClure MO, Abrahams VM, Wheelhouse N, Jabbour HN, Critchley HO, Entrican G *et al.* Chlamydia trachomatis Infection Increases Fallopian tube PROKR2 via TLR2 and NFkappaB activation resulting in a microenvironment predisposed to ectopic pregnancy. *Am J Pathol* 2011;**178**:253–260.

Sivalingam VN, Duncan WC, Kirk E, Shephard LA, Horne AW. Diagnosis and management of ectopic pregnancy. *J Fam Plann Reprod Health Care* 2011;**37**:231–240.

Stephens LE, Sutherland AE, Klimanskaya IV, Andrieux A, Meneses J, Pedersen RA, Damsky CH. Deletion of beta 1 integrins in mice results in inner cell mass failure and peri-implantation lethality. *Genes Dev* 1995;**9**:1883–1895.

Sulz L, Valenzuela JP, Salvatierra AM, Ortiz ME, Croxatto HB. The expression of alpha(v) and beta3 integrin subunits in the normal human Fallopian tube epithelium suggests the occurrence of a tubal implantation window. *Hum Reprod* 1998;**13**:2916–2920.

Taylor HS, Vanden Heuvel GB, Igarashi P. A conserved Hox axis in the mouse and human female reproductive system: late establishment and persistent adult expression of the Hoxa cluster genes. *Biol Reprod* 1997;**57**:1338–1345.

Tei C, Maruyama T, Kuji N, Miyazaki T, Mikami M, Yoshimura Y. Reduced expression of alphavbeta3 integrin in the endometrium of unexplained infertility patients with recurrent IVF-ET failures: improvement by danazol treatment. *J Assist Reprod Genet* 2003; **20**:13–20.

Varma R, Gupta J. Tubal ectopic pregnancy. *Clin Evid (Online)* 2009; **20**:pii: 1406.

Yang JT, Rayburn H, Hynes RO. Cell adhesion events mediated by alpha 4 integrins are essential in placental and cardiac development. *Development* 1995;**121**:549–560.